Discrimination of Single- and Multi-Source Corona Discharges using Deep Residual Network

Moein Borghei
The Bradley Department of Electrical and Computer Engineering
Virginia Tech
Blacksburg, VA, USA
moeinrb@vt.edu

Mona Ghassemi
The Bradley Department of Electrical and Computer Engineering
Virginia Tech
Blacksburg, VA, USA
monag@vt.edu

***Abstract*— Partial discharge (PD) is a major aging factor in insulation systems. The first step toward ensuring the health of insulation systems is the identification of PD sources. This would enable the system operator to take proper actions before the occurrence of the final breakdown. This fundamental study targets building and training a deep residual neural network (ResNet) model to detect and discriminate single and multiple sources of corona discharge that are acting simultaneously. The input of the ResNet model is the actual PD measurements under atmospheric pressure for seven electrode configurations: four single-source and three double-source configurations which expands from weakly nonuniform to extremely nonuniform electric field distribution. In this study, the measurement data are converted into standardized phase-resolved PD (PRPD) images that would be further used as input to the optimized ResNet model. The validation of the 62-layer deep neural network is evaluated through 30% randomly chosen images from the original dataset.**

Keywords—Artificial intelligence, corona discharge, deep learning, partial discharge, residual neural network.

I. INTRODUCTION

A crucial part of any electrical system is the insulation system that separates the conductive parts and prevents the short circuit between them. Therefore, the proper operation of insulating material ensures the reliable operation of the equipment. The dielectric (insulating material) can be in any state (e.g., gas, liquid, or solid).

A primary aging factor in dielectrics is partial discharge (PD) [1-7]. According to the standard of the International Electrotechnical Commission (IEC) 60270 [8], "Partial discharge (PD) is a localized electrical discharge that only partially bridges the insulation between conductors, and which may or may not occur adjacent to a conductor."

Three types of PDs can happen depending on the medium and insulation quality. If there is inclusion or cavity inside a solid/liquid dielectric, an "internal discharge" can happen. If there are protrusions or imperfections at the surface of the dielectric or electrode, it is likely that "surface discharge" happens. Under an inhomogeneous electric field around an electrode in gas, a local and continuous discharge may happen which is known as "corona discharge" [9].

Four types of internal PD modeling, in sequential order from first to last developed, are three-capacitance (abc), induced charge concept (ICC) [10], finite element analysis (FEA) [11-19], and Multiphysics models [20, 21].

PD testing has a history of almost 100 years and has played a pivotal role in the diagnosis and analysis of this phenomenon. As a result of PD measurements, several indices and figures have been defined to facilitate PD analysis. One of these figures is the phase-resolved PD pattern (PRPD) that has helped engineers to identify the type of discharges simply by looking at their PRPD pattern. For instance, in the case of internal discharges, PRPD has a pattern like "rabbit-ear". A research gap lies in the possibility of identifying the sources of discharge from the PRPD pattern. The challenge, however, is due to the visibility of differences by human eyes, specifically for short-term data.

With the proliferation of PD measurement units, an extensive amount of PD signals is available. Extracting the useful information from these invaluable resources manually may not be possible. Therefore, the machine learning approaches can help us to perform feature extraction and classification automatically. Machine learning algorithms are fed by a dataset to learn from the data and make proper decisions about a parameter (or more). However, typical machine learning approaches require the human user to provide the features needed for classification. Recently, a branch of machine learning – called deep learning (DL) – has received substantial attention due to its independence from feature engineering by the user. Especially, DL has achieved significant advancements in the case of image recognition and classification [22].

DL models can extract and integrate features at different levels (low, mid, and high) and in different numbers to capture as much variance as possible in a time-efficient manner [23]. There has much research on the impact of network depth on the ability of DL models to achieve higher precision [24]. Evidence has proven that DL models can be effectively trained and tested by challenging image datasets through a high number of stacked layers [25]. This is beneficial for the case of classification of PRPD images as they are not easy to classify.

However, the difficulty of training increases by the depth of the neural network. In [26], a deep residual learning framework is proposed to facilitate the training of deep networks. In this approach, the layers learn residual functions with reference to input layers (instead of typical unreferenced versions).

In this paper, we target the classification of a dataset consisting of seven discharge sources including single- and double-source corona discharges. After presenting the measurement results for these test configurations, we deploy a residual network (ResNet) model and optimize to discriminate these corona discharge sources.

2021 IEEE Electric Ship Technologies Symposium (ESTS) | 978-1-7281-8426-5/21/$31.00 ©2021 IEEE | DOI: 10.1109/ESTS49166.2021.9512372

The rest of the paper is as follows: in section II, we present the experimental setup and the testing procedure along with the voltage source characteristics. In section III, the architecture of the ResNet model is introduced and discussed. Also, the production and processing of input images are explained. The results of the deep learning approach are presented in section IV. Finally, section V concludes the paper.

II. Experimental Setup

The experimental setup in this study provides the input to the ResNet model through various test cells (i.e., electrode configuration). The electrode configurations considered in this study are sphere-sphere, sphere-plane, needle-needle, and needle-plane. The first two configurations lead to weakly nonuniform and the next two configurations lead to extremely nonuniform electric field distributions which is the common case in real-world applications. Besides these four single sources of corona discharge, three double sources of corona discharge will be investigated.

Fig. 1 shows the experimental setup. A standardized test procedure is used for all these scenarios to generate comparative datasets. The test procedure is based on IEC 61287-1 [27] (Fig. 2). The only modification of this procedure is in the initial rise time of voltage that 20 s instead of 10 s. The gap distance and the voltage peak (U_m) in all cases are 2 cm and 6 kV, respectively. Note that the PRPD images are extracted from the 60-second period in which the test cell undergoes the highest voltage.

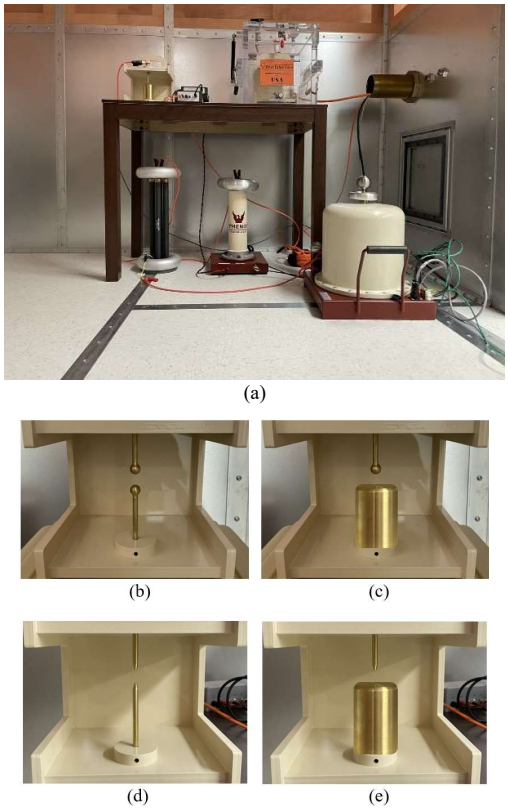

Fig. 1. The experiment system: (a) test setup, (b) sphere-sphere, (c) sphere-plane, (d) needle-needle, and (e) needle-plane electrode configuration.

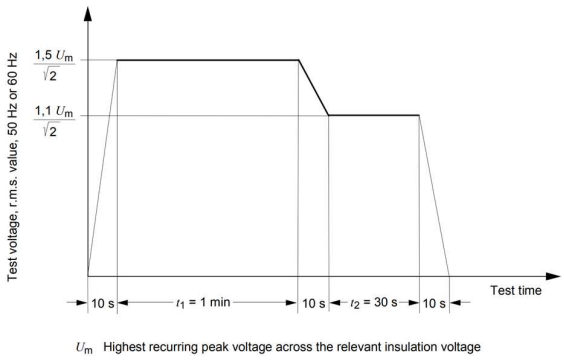

Fig. 2. The test procedure defined in standard IEC 61287 [27].

The PRPD patterns of all seven test samples are shown in Fig. 3. While a slight difference is observable after the whole pattern is formed, it is not a trivial task to identify the source of PD in the early stages. Also, the difference between the patterns of a single-source discharge (e.g. sphere-plane) and a double-source discharge (e.g. needle-needle and sphere-plane) may not be visible while a data analytics tool can accurately discriminate them. Hence, this paper targets the discrimination of different single- and double-source discharges using deep neural networks to enhance awareness about the insulation system conditions.

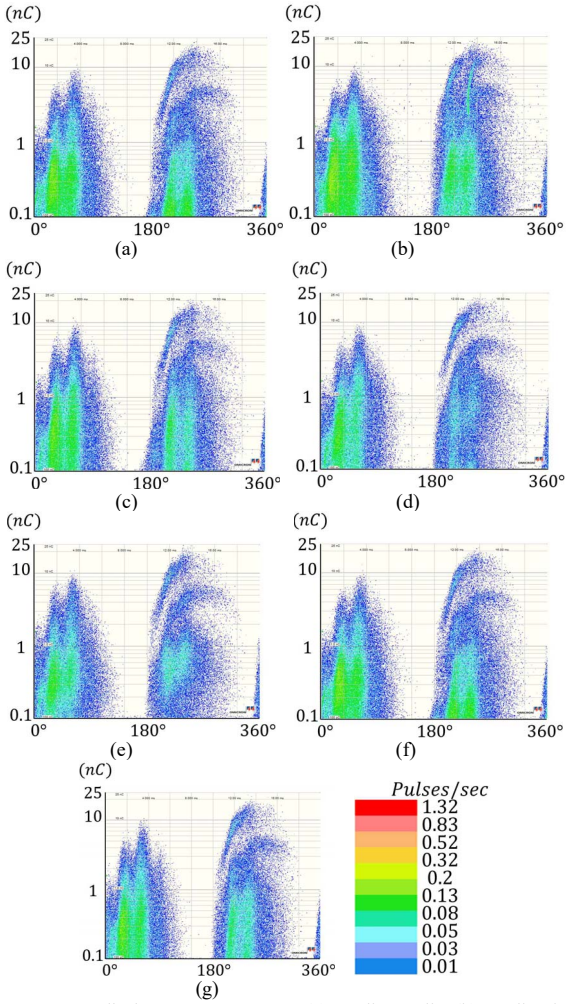

Fig. 3. Corona discharge PRPD pattern: (a) needle-needle, (b) needle-plane, (c) sphere-plane, (d) sphere-sphere, (e) sphere-sphere and needle-needle, (f) sphere-sphere and needle-plane, and (g) needle-needle and sphere-plane.

III. ResNet Architecture

The measured PD signals are used to train a deep residual network model. The inputs of the model will be in form of the phase-resolved PD (PRPD) patterns. However, the PRPD images need to be preprocessed before being used in the ResNet model.

The preprocessing stage is implemented in MATLAB and follows these steps: (1) Importing raw data to MATLAB, (2) filtering discharges that are too small in magnitude (those that have charge magnitude below 0.5 nC), (3) defining proper time interval for generating PRPD patterns, (4) generating PRPD pattern in the desired size and under a unified x, and y range. Fig. 4 shows a sample PRPD pattern. Note that since the range of the x-axis and y-axis are both unified, we have omitted the x and y axes to prevent the exhaustion of the ResNet model with unimportant image aspects. The y-axis extends from 0.5 nC to 25 nC which is the highest PD magnitude observed in all cases. The sampling rate is 10 (60 Hz) cycles per PRPD plot meaning that each generated image represents ~167 ms of the data. The PRPD images are produced at the rate of 20 patterns per second. This gives about 1200 images per electrode configuration and a total of 8400 images. The images are all in greyscale and 32×32 pixels.

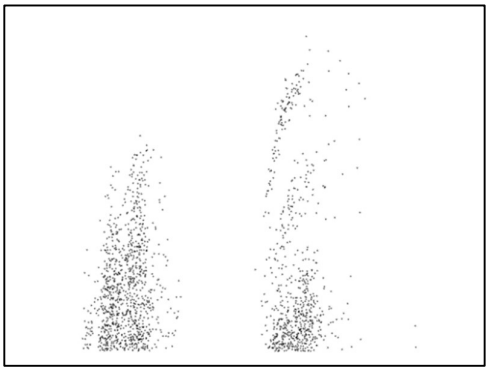

Fig. 4. A sample PRPD image used as ResNet model input.

The PRPD pixels are normalized and the classes/labels (which are the type of discharge) are converted into a one-hot vector for adaptability to the ResNet model. The model will be trained with each PD source separately and then, the test data of the superimposition of these sources will demonstrate the performance of the model. The ability of the model to discriminate multiple PD sources will be evaluated using a test dataset (30% of the original dataset is randomly chosen).

— *Residual Network Concept*

In residual networks, every few weighted layers, an identity mapping is performed by adding the output of a previous layer to the next layer after skipping connections. This concept is shown in Fig. 5. In this figure, the identity mapping occurs after 2 layers, but this number can vary depending on the problem. Normally, the input $\mathbf{x}$ is multiplied by the two weighted layers to achieve output $\boldsymbol{y} = \boldsymbol{\mathcal{F}}(\mathbf{x})$; however, in the residual block shown in Fig. 5, the output of the weighted layers are summed up with the identity mapping of the input: $\boldsymbol{y} = \boldsymbol{\mathcal{F}}(\mathbf{x}) + \mathbf{x}$. This helps to mitigate the vanishing gradient problem. Moreover, the addition of identity mapping ensures that the deeper layers perform at least as good as the previous layers. In comparison with CNNs, ResNet has fewer filters and is relatively less complex in training.

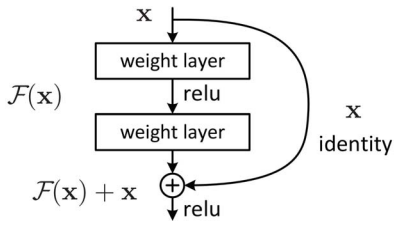

Fig. 5. A sample residual block [26].

— *Architecture*

The architecture of the deep residual network designed for this study is shown in Fig. 6. The idea behind ResNet is to use network layers to fit a residual mapping instead of directly trying to fit a desired underlying mapping (see the residual block). In the design of convolutional layers, the layers have the same number of filters as the output feature size. Also, to maintain the computational complexity relatively constant, the number of filters has an opposite relationship with the feature map size. This means that the number of filters will be doubled if the feature map size is cut in half. Thus, the number of filters is doubled and each dimension is halved periodically.

Also, there are transition layers between residual blocks (a 1x1 2D convolutional layer with the stride of 2) to shrink the number of feature maps and make the model more compact. Also, at the end of each transition layer, a dropout layer is placed to prevent overfitting (the dropout rate is 0.4). After each convolutional layer, batch normalization is placed followed by a rectified linear unit (ReLU) activation function.

At the end of the residual blocks, we conduct down-sampling by having convolutional layers that have a stride of 2. The network concludes by a global average pooling layer and a 7-class fully connected layer with softmax. The total number of convolutional layers in this model is 62 assuming that the repetition of double residual convolutional layers in each residual block is n=10.

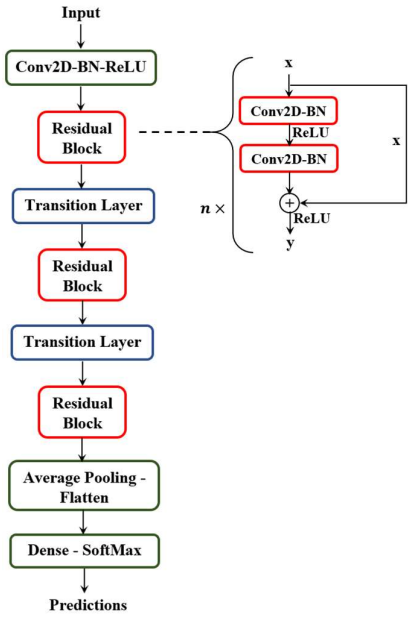

Fig. 6. The proposed ResNet architecture.

IV. Results

The proposed ResNet model is developed in Python using Tensorflow (Keras) library. The model has 62 weighted layers while the batch size and number of epochs are 128 and 200, respectively. However, an early stopping (with a 10 epoch patience concerning vanishing loss function) may end the iterations before reaching 200 epochs.

The loss function is categorical cross-entropy and the Adam method is adopted as an optimizer. The training and testing accuracy obtained by the ResNet model is 98.9% and 79.7%, respectively. This shows great potential for deep learning methods to accurately discriminate the different corona discharge sources using less than 100 iterations.

In Fig. 7, the training and validation accuracy is plotted versus. This can help us to monitor overfitting. While at the training level, the labeling of sources is done with almost 100% accuracy, the validation is 15%-50% less accurate. As the number of iterations increases, the validation accuracy tends to saturate giving a satisfactory value of ~80%.

Fig. 7. The training vs validation accuracy.

In Fig. 8, a sample PRPD image is shown which is followed by its feature map after the first convolutional layer with 16 filters. This figure demonstrates how different aspects of the pattern are detected by each filter. The high accuracy level achieved by this method is representative of the efficacy of the aggregated filters in the ResNet model. As the model goes deeper, a higher level of information could be extracted by the filters.

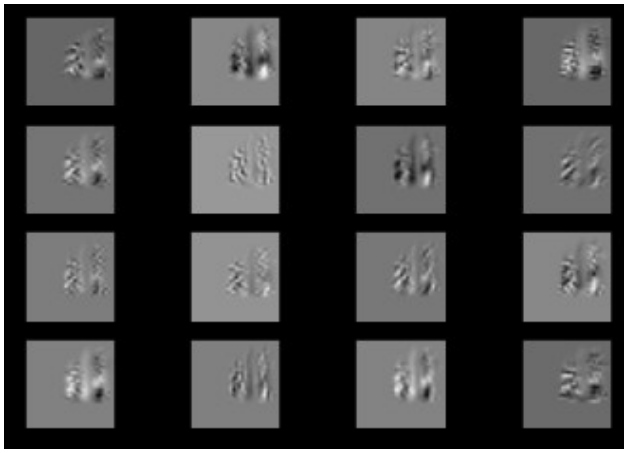

Fig. 8. The feature map of a sample image after the first convolutional layer.

V. Conclusion

In this paper, we proposed, designed, and optimized a deep residual neural network for the discrimination of corona discharge sources. The input of the model was PD measurements performed in 7 different scenarios including three double-source and four single-source test configurations. The measurement data was processed and standardized to prepare a large set of PRPD images. While it is not easy to manually discriminate the sources of corona discharge – especially with short-term data –, neural networks can help us to automatically do that within a short period. The very deep ResNet model developed in this study could tackle the problem using 62 convolutional layers and achieve about ~80% accuracy.

Acknowledgment

This work was supported in part by the Office of Naval Research (ONR) under Award N00014-19-1-2343 and in part by the National Science Foundation (NSF) under Award 1942540.

References

[1] M. Borghei and M. Ghassemi, "Insulation materials and systems for more and all-electric aircraft: A review identifying challenges and future research needs," IEEE Trans. Transport. Electrific., 2021, Early Access, DOI: 10.1109/TTE.2021.3050269.

[2] B. Zhang, M. Ghassemi, and Y. Zhang "Insulation materials and systems for power electronics modules: A review identifying challenges and future research needs," IEEE Trans. Dielectr. Electr. Insul., vol. 28, no. 1, pp. 290–302, Feb. 2021.

[3] M. Ghassemi, "Accelerated insulation aging due to fast, repetitive voltages: A review identifying challenges and future research needs," IEEE Trans. Dielectr. Electr. Insul., vol. 26, no. 5, pp. 1558–1568, Oct. 2019.

[4] M. Ghassemi, "Electrical insulation weaknesses in wide bandgap devices," in *Simulation and Modelling of Electrical Insulation Weaknesses in Electrical Equipment*, R. Albarracin Ed., London, U.K.: IntechOpen, 2018, pp. 129–149.

[5] M. Ghassemi, "Partial discharge measurements, failure analysis, and control in high-power IGBT modules," High Voltage, vol. 3, no. 3, pp. 170–178, Sep. 2018.

[6] M. Ghassemi, "High power density technologies for large generators and motors for marine applications with focus on electrical insulation challenges," High Voltage, vol. 5, no. 1, pp. 7-14, Feb. 2020.

[7] A. Barzkar and M. Ghassemi, "Electric power systems in more and all electric aircraft: a review," *IEEE Access*, vol. 8, pp. 169314–169332, Sept. 2020.

[8] IEC 60270, High-voltage test techniques – Partial discharge measurements, 2000.

[9] E. Kuffel, W. Zaengl, and J. Kuffel, "High voltage engineering fundamentals," Oxford: Newnes, Second Edition, 2000.

[10] M. Borghei, M. Ghassemi, J. M. Rodríguez-Serna, and R. Albarracín-Sánchez, "A finite element analysis and an improved induced charge concept for partial discharge modeling," IEEE Trans. Power Del., 2020, Early Access. DOI: 10.1109/TPWRD.2020.2991589

[11] M. Borghei, M. Ghassemi, B. Kordi, P. Gill, and D. Oliver, "A finite element analysis model for internal partial discharges in an air-filled, cylindrical cavity inside solid dielectric," IEEE Electrical Insulation Conference (EIC), June 7–21, 2021.

[12] M. Borghei and M. Ghassemi, "A finite element analysis model for partial discharges in silicone gel under a high slew rate, frequency square wave voltage in low-pressure conditions," Energies, vol. 13, no. 9, p. 2152, May 2020.

[13] M. Borghei and M. Ghassemi, "Partial discharge analysis under high-frequency, fast-rise square wave voltages in silicone gel: A modeling approach," Energies, vol. 12, 4543, 2019.

[14] M. Borghei, M. Ghassemi, B. Kordi, P. Gill, and D. Oliver, "Modeling and measurement of internal partial discharges in voids artificially made within 3D-printed polylactic acid (PLA) block," IEEE Electric

Ship Technologies Symposium (ESTS), Arlington, VA, USA, Aug. 3-6, 2021.

[15] M. Borghei and M. Ghassemi, "Characterization of partial discharge activities in WBG power modules under low-pressure condition," IEEE Conference Electrical Insulation Dielectric Phenomena (CEIDP), East Rutherford, NJ, USA, pp. 297-300, Oct. 18-22, 2020.

[16] M. Borghei and M. Ghassemi, "Investigation of low-pressure condition impact on partial discharge in micro-voids using finite-element analysis," IEEE Energy Conversion Congress & Expo. (ECCE), Detroit, MI, USA, pp. 3293-3298, Oct. 11-15, 2020.

[17] M. Borghei and M. Ghassemi, "Effects of low–pressure condition on partial discharges in WBG power electronics modules," IEEE Electrical Insulation Conference (EIC), Knoxville, TN, USA, pp. 199-202, June 22–July 06, 2020.

[18] M. Borghei and M. Ghassemi, "Partial discharge finite element analysis under fast, repetitive voltage pulses," IEEE Electric Ship Technologies Symposium (ESTS), Arlington, VA, USA, pp. 324-328, Aug. 13-19, 2019.

[19] M. Borghei and M. Ghassemi, "Finite element modeling of partial discharge activity within a spherical cavity in a solid dielectric material under fast, repetitive voltage pulses," IEEE Electrical Insulation Conference (EIC), Calgary, Canada, pp. 34-37, June 16-19, 2019.

[20] G. Callender, T. Tanmaneeprasert, and P. L. Lewin, "Simulating partial discharge activity in a cylindrical void using a model of plasma dynamics," *J. Phys. D: Appl. Phys.*, vol. 52, no. 5, 2019.

[21] G. Callender, I. O. Golosnoy, P. Rapisarda, and P. L. Lewin, "Critical analysis of partial discharge dynamics in air filled spherical voids," *J. Phys. D: Appl. Phys.*, vol. 51, no.12, 2018.

[22] A. Krizhevsky, I. Sutskever, and G. Hinton, "Imagenet classification with deep convolutional neural networks," Conf. on Neural Information Processing Systems (NIPS), 2012.

[23] M. D. Zeiler and R. Fergus. "Visualizing and understanding convolutional neural networks," European Conf. on Computer Vision (ECCV), 2014.

[24] K. Simonyan and A. Zisserman, "Very deep convolutional networks for large-scale image recognition," Int. Conf. Learning Representations (ICLR), 2015.

[25] C. Szegedy et al., "Going deeper with convolutions," IEEE Conf. Computer Vision and Pattern Recognition (CVPR), Boston, MA, USA, 2015, pp. 1–9.

[26] K. He, X. Zhang, S. Ren and J. Sun, "Deep residual learning for image recognition," IEEE Conf. Computer Vision and Pattern Recognition (CVPR), Las Vegas, NV, USA, 2016, pp. 770–778.

[27] IEC 61287-1: "Railway applications – power converters installed on board rolling stock – part 1: characteristics and test methods," Edition 3.0, 2014.